

Ballistic and diffusive transport of energy and heat in metals

Y. Ezzahri* and A. Shakouri†

Department of Electrical Engineering, University of California–Santa Cruz, Santa Cruz, California 95064, USA

(Received 2 February 2009; published 26 May 2009)

We exploit a recently developed formalism to study the temporal behavior of the energy and heat transport in metals. This formalism shows the transition between ballistic and diffusive regimes and it highlights some interesting effects such as oscillations in the energy transport at very short-time scales. The energy relaxation of the conduction-band electrons in metals is considered to be governed by electron-phonon scattering, and the scattering time is taken to be averaged over the Fermi surface. The analysis separates the diffusive and the nondiffusive contributions to the heat transport. While the diffusive contribution shows an almost exponentially decaying behavior with time, the nondiffusive part shows a damped oscillating behavior. The origin of this oscillation will be discussed as well as the effect of the ambient temperature on the dynamics of the energy modes transport.

DOI: 10.1103/PhysRevB.79.184303

PACS number(s): 72.15.Eb, 72.15.Cz, 44.10.+i

I. INTRODUCTION

Development of high-power short-pulse laser sources with a pulse width in the sub-ps range has provided an opportunity to study the propagation of energy and heat at very short-time scales; it has also created many applications in thin-film analysis or in material processing. Ultrafast laser sources have made possible the study of many interesting fundamental physical phenomena in condensed matter such as electrons transitions in semiconductors,^{1,2} electron-phonon coupling in metals,^{3–7} and electron dynamics in semiconductor superlattices.^{8,9} Shorter laser pulses in the sub-fs range have recently opened the field to explore electronic interactions within the atom itself.¹⁰

Energy and heat transport during short-pulse laser heating of solid materials is an important phenomenon that needs to be fully understood to better control the abundant applications in which short-pulse lasers are used. The question of energy and heat transport mechanisms at short-time scales is the basis of numerous theoretical and experimental papers. From the microscopic point of view, energy deposits into and propagates through a material in different ways, depending on the excitation, the structure of the material, and the nature of the energy carriers. At short-time scales, Fourier's law becomes invalid and many non-Fourier energy conduction models have been developed to overcome problems associated with Fourier's model (e.g., infinite speed of propagation of heat).^{11–14} Most importantly, the distinction between diffusive and nondiffusive (ballistic) regimes of energy transport becomes very relevant at these short-time scales.¹⁵

Recently, Shastry¹⁶ has developed a formalism based on linear theory to describe coupled charge and energy transport in a solid material system. The formalism is general and gives a set of equations for the electrothermal transport coefficients in the frequency-wave vector domain. One of the most important results of this formalism is the introduction of response functions describing the change in energy density, charge density, and the currents arising from the input excitation (coefficients M_1 , M_2 , N_1 , and N_2 as defined in the reference article¹⁶). Among these response functions, N_2 is of particular interest since this function gives a measure of the change in energy density and hence temperature at various points in the system in response to the applied excitation at

the top free surface of the system, and as such represents the energy (heat) Green's function of the system.

The objective of the current work is to analyze the transient energy and heat transport in metals occurring after application of a heating source at the top free surface of the metal in the frame work of the above mentioned formalism. We will show how this formalism shows the transition between ballistic and diffusive regimes and it highlights some interesting effects such as oscillations in the energy transport at very short-time scales.

II. THEORY

The starting point of our analysis is the Shastry-Green function N_2 in the decoupled limit for metals. According to Shastry's work,¹⁶ the coupling factor ξ between charge and energy modes can be expressed using the high-frequency value of the thermoelectric figure-of-merit Z^*T ,

$$\xi = \frac{Z^*T}{Z^*T + 1}. \quad (1)$$

Here Z^* is the high-frequency limit of the Seebeck coefficient square times the electrical conductivity divided by the thermal conductivity. It is well known however; that metals are very poor thermoelectric materials with a very low ZT .¹⁷ The decoupled limit is thus justified. By turning off the coupling between the charge and energy modes ($\xi=0$), N_2 can be expressed as

$$N_2(\omega, q) = \frac{-i + \tau_q \omega}{\omega + i\tau_q \omega^2 - iD_e q^2}. \quad (2)$$

We should note here that Eq. (2) is given for an arbitrary applied power function $P(t)$ at the top free surface of a metal. This expression is a generalization of the one given by Shastry in the case of a periodic power function.¹⁶ ω is the circular frequency, q is the electron wave vector, D_e is the electronic thermal diffusivity, and τ_q is the total electron-scattering time, which, in general, is a function of q . Remarkably, in the case of a q -independent τ_q , the form of N_2 in the frequency-wave vector domain resembles the expression of the energy density change at the top free surface of



FIG. 1. (Color online) Schematic of the metal being excited by a laser delta pulse at its free top surface ($x=0$).

the metal, one would have derived using Cattaneo's model and solving the energy density equation for electrons in the case of a delta power excitation applied to the same surface. It is straightforward to convert the heat equation for electrons to an energy density equation using the relation between the electronic energy density δK and the electronic temperature T_e : $\delta K(t, x) = \frac{1}{2} C_e(T_e) T_e(t, x)$ where C_e is the electronic specific heat per unit volume. As we shall show later in the discussion, the difference in the behavior between Cattaneo's model and Shastry's model is due to the band cutoff effect in the case of N_2 . Cattaneo's model can be viewed as the continuous limit of N_2 .

In the following we consider a one-dimensional energy transport problem, in which case we assume the top metal free surface being excited by an input laser pulse of power $P(t)$. The one-dimensional approximation is reasonable at short-time scales considering the ratio of the size of the laser-pulse spot to the diffusion length which in this case is small on the order of the optical penetration depth. The later quantity depends on the wavelength of the laser, but it is less than 10 nm over a large range of wavelengths for most metals.¹⁸ The optical penetration depth becomes even much shorter on the order of 1 nm if very short wavelengths are used (e.g., UV with a frequency lower than the plasmon frequency of the corresponding metal).¹⁸ This is very useful since it validates the assumption we are making of a surface excitation. Figure 1 shows a schematic of the metal under excitation, where the laser pulse excites the top free surface ($x=0$).

After excitation of the top metal free surface with a power input $P(t)$, the change of the energy density in the frequency-wave vector domain $\delta K(\omega, q)$ can be expressed as¹⁶

$$\delta K(\omega, q) = N_2(\omega, q) \times \bar{P}(\omega), \quad (3)$$

where $\bar{P}(\omega)$ is the Fourier transform of $P(t)$ in the frequency domain. The change in the energy density at the top free surface of the metal as function of time is obtained by a double inverse Fourier transforms with respect to ω and q ,

$$\delta K(t, 0) = \frac{1}{(2\pi)^2} \int_{-\pi/a}^{\pi/a} \left[\int_{-\infty}^{+\infty} N_2(\omega, q) \bar{P}(\omega) e^{i\omega t} d\omega \right] dq. \quad (4)$$

The integration over q is taken over the first Brillouin zone (FBZ) in the one-dimensional case, where "a" refers to the lattice constant of the metal. The power source $P(t)$ can be of any form, but we will limit our study to the ideal case of a Dirac delta function $P(t) = P_0 \times \delta(t)$ in order to capture the intrinsic evolution of the energy density $\delta K(t, 0)$ as a function of time: *the temporal behavior of the energy density Green's function at the top free surface of the metal.*

The integral within the square brackets in Eq. (4) can be analytically calculated using the residue theorem. As a matter of fact, the integrand of this integral has two single poles that lie in the upper complex half plane. These poles are given, respectively, by

$$\omega_{\pm} = i \frac{1 \pm \sqrt{1 - 4D_e \tau_q q^2}}{2\tau_q}. \quad (5)$$

A straightforward calculation of the residues at these two single poles leads to

$$P_0 \int_{-\infty}^{+\infty} N_2(\omega, q) e^{i\omega t} d\omega = 2\pi P_0 e^{-t/2\tau_q} \left[ch\left(\frac{R_q t}{2\tau_q}\right) + \frac{sh\left(\frac{R_q t}{2\tau_q}\right)}{R_q} \right]; \quad (6)$$

$$R_q = \sqrt{1 - 4D_e \tau_q q^2}.$$

Equation (4) can then be re-expressed as

$$\delta K(t, 0) = \frac{P_0}{2\pi} \int_{-\pi/a}^{\pi/a} e^{-t/2\tau_q} \left[ch\left(\frac{R_q t}{2\tau_q}\right) + \frac{sh\left(\frac{R_q t}{2\tau_q}\right)}{R_q} \right] dq. \quad (7)$$

Up to now, the equations are completely general regardless the dependence of the relaxation time on the wave vector. Electron relaxation in the conduction band of metals is governed by two scattering processes; (i) electron-electron scattering process and (ii) electron-phonon scattering process.¹⁹ In most metals, the second process is generally the dominant one and the transport of energy by phonons can be neglected. Using the fact that electrons and phonons in a metal can be characterized by different temperatures, it has been shown that scattering of electron by phonons can be either elastic or inelastic, and the relaxation time is inversely proportional to the lattice temperature.^{4,20-22} In the following, we consider the case of a constant relaxation time $\tau_q = \tau_F$, which we consider to be the average scattering time of electrons over the Fermi surface of the metal. Equation (7) can be split into two parts, depending on the sign of the argument of R_q . We can write it down as

$$\delta K(t, 0) = \delta K^<(t, 0) + \delta K^>(t, 0),$$

$$\delta K^<(t, 0) = \frac{P_0}{\pi} e^{-t/2\tau_F} \int_0^{q_0} \left[ch\left(\frac{R_q t}{2\tau_F}\right) + \frac{sh\left(\frac{R_q t}{2\tau_F}\right)}{R_q} \right] dq, \quad (8a)$$

$$\delta K^>(t, 0) = \frac{P_0}{\pi} e^{-t/2\tau_F} \int_{q_0}^{q_m} \left[\cos\left(\frac{\bar{R}_q t}{2\tau_F}\right) + \frac{\sin\left(\frac{\bar{R}_q t}{2\tau_F}\right)}{R_q} \right] dq, \quad (8b)$$

$$q_m = \frac{\pi}{a}; \quad q_0 = \frac{1}{2\sqrt{D_e \tau_F}} \quad \text{and} \quad \bar{R}_q = \sqrt{4D_e \tau_F q^2 - 1}.$$

The first part in Eq. (8) describes the diffusive contribution and is exponentially decaying as function of time. On the

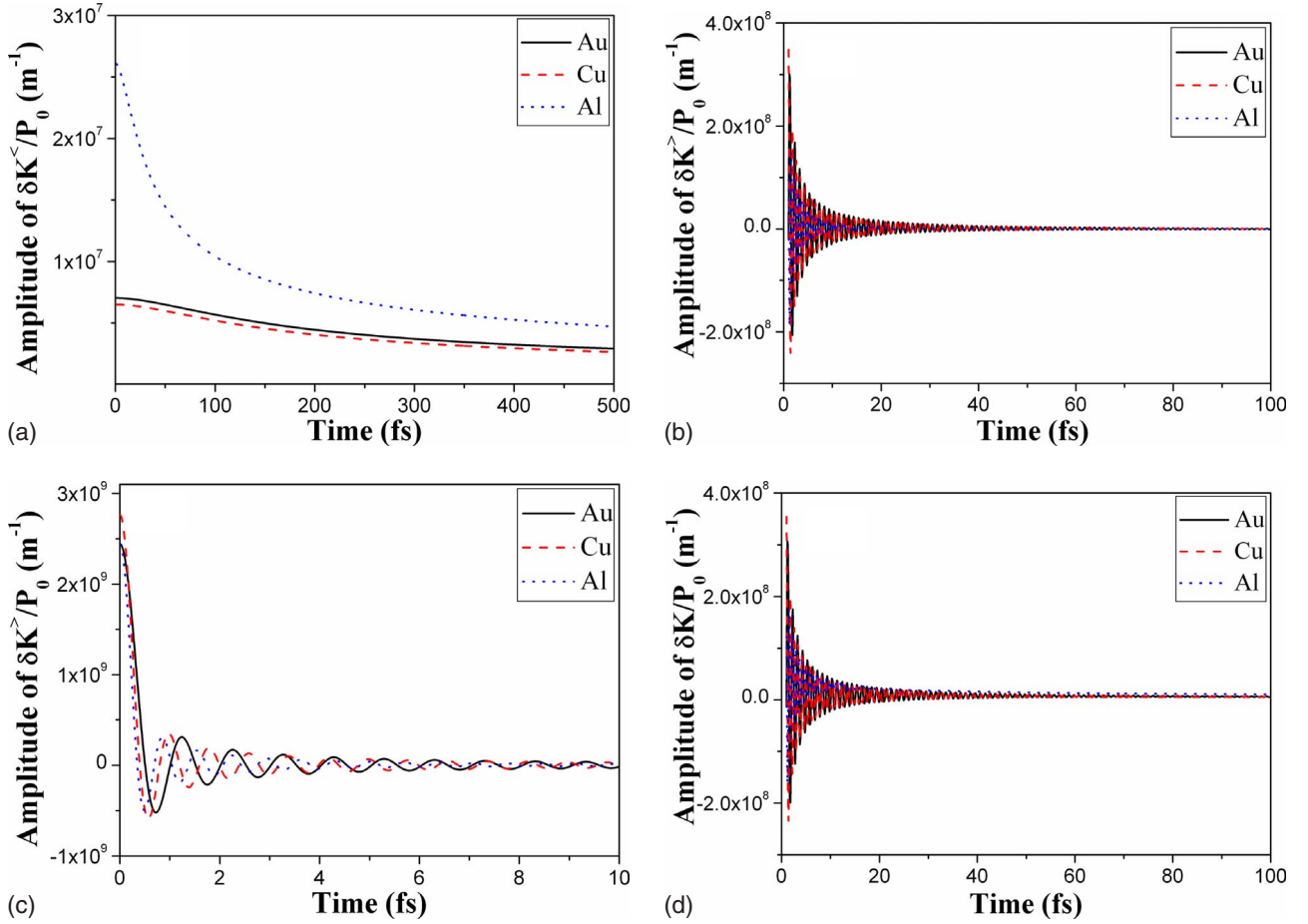


FIG. 2. (Color online) Temporal behavior of the energy density Green's function at the top free surface of different metals at room temperature: (a) Eq. (8a), (b) Eq. (8b), (c) Zoom of figure (b). (d) Whole integral in Eq. (8).

other hand, the second part describes the nondiffusive part. It is interesting to notice the oscillating character of the integrand in Eq. (8b) which will result after integration over q in a damped oscillating behavior.

In the section below, we will discuss the fundamental origin of the oscillating behavior that characterizes the nondiffusive contribution, as well as the effect of the ambient temperature on the period and damping of these oscillations.

III. RESULTS AND DISCUSSION

At electron temperatures $T_e \leq T_F$, where T_F is the Fermi temperature, the electron thermal conductivity is given by $\beta_e = C_e v_F^2 \tau_F / 3$,¹⁹ where v_F is the Fermi velocity, τ_F is the scattering relaxation time of electrons averaged over the Fermi surface of the metal, and $C_e(T)$ is the temperature-dependent specific heat per unit volume of the electronic system. $C_e(T) = \pi^2 / 3 k_B^2 g(\varepsilon_F) T = \gamma T$ where $g(\varepsilon_F)$ is the electronic density of states at the Fermi energy ε_F . The thermal diffusivity of the electronic system in the conduction band of the metal is then given by

$$D_e = \frac{\beta_e}{C_e} = \frac{v_F^2 \tau_F}{3}. \quad (9)$$

In Fig. 2, we have plotted the temporal behavior of the different contributions to the energy density Green's function at the top free surface of different metals at room temperature $T=300$ K, as given by Eqs. (8a) and (8b). More specifically the vertical axis in these figures represents the quantity $\delta K(t, 0) / P_0$ which has the unit of the absorption coefficient (m^{-1}). The higher is this quantity the higher is the energy density and hence the temperature at the top free surface of the metal. Values of the scattering relaxation time τ_F are estimated based on the values of the electrical resistivity using Drude theory.¹⁹ Table I summarizes these values as well as the values of the Fermi velocities and the electronic thermal diffusivities of the different metals at room temperature.

TABLE I. Properties of the different metals used in the calculation at room temperature.

Metal	Lattice constant (Å)	Relaxation time τ_F (fs)	Fermi velocity v_F (10^6 m/s)	Electronic thermal diffusivity D_e (m^2/s)
Au	4.08	28	1.4	0.0183
Cu	3.61	27	1.57	0.0222
Al	4.05	5.2	2.03	0.0071

The left side of the integral as described by Eq. (8a) shows a smooth decaying behavior as a function of time which is almost an exponential [Fig. 2(a)]. This behavior is characteristic of the diffusive regime of the heat transport by electrons. On the other hand, the right side of the integral shows an oscillating behavior as a function of time [Fig. 2(b)]. The oscillations are damped out exponentially with

time. Figure 2(c) shows a zoom of the oscillations over the first 10 fs. The period of these fast oscillations can be estimated using Eq. (8b) as follows.

For values of the wave vector q between q_0 and q_m , we can with a very good approximation neglect 1 in the argument of \bar{R}_q , the latter becomes then $\bar{R}_q \approx 2q\sqrt{D_e\tau_F}$, and Eq. (8b) can be rewritten as

$$\delta K^>(t,0) = \frac{P_0}{\pi} e^{-t/2\tau_F} \int_{q_0}^{q_m} \left[\cos\left(q\sqrt{\frac{D_e}{\tau_F}}t\right) + \frac{\sin\left(q\sqrt{\frac{D_e}{\tau_F}}t\right)}{2q\sqrt{D_e\tau_F}} \right] dq. \tag{10}$$

This integral can be calculated analytically, the result of which is given by

$$\delta K^>(t,0) = \frac{P_0}{\pi} e^{-t/2\tau_F} \left[\frac{\sin\left(q_m\sqrt{\frac{D_e}{\tau_F}}t\right) - \sin\left(\frac{t}{2\tau_F}\right)}{\sqrt{\frac{D_e}{\tau_F}}t} + \frac{\text{Si}\left(q_m\sqrt{\frac{D_e}{\tau_F}}t\right) - \text{Si}\left(\frac{t}{2\tau_F}\right)}{2\sqrt{D_e\tau_F}} \right], \tag{11}$$

where Si represents the Sine integral function given by $\text{Si}(z) = \int_0^z \frac{\sin(x)}{x} dx$.²³

As we can see in this equation, the result contains two main periods, $\theta_F = 2\pi/q_m\sqrt{D_e/\tau_F}$ and $\theta_S = 4\pi\tau_F$ where θ_F and θ_S describe the fast and slow oscillation periods, respectively. Replacing the expression of q_m and D_e into θ_F allows us to write the fast oscillation period as

$$\theta_F = 2\sqrt{3} \frac{a}{v_F}. \tag{12}$$

The fast oscillation is function only of the lattice constant of the metal and its Fermi velocity, and is independent of the scattering relaxation time of the electrons in the conduction band. For almost all metals $a \sim 4 \text{ \AA}$ and v_F is of the order of $1.4 \times 10^6 \text{ m/s}$, a simple application of Eq. (12) shows then that the period of this first oscillation is very small $\theta_F \approx 1 \text{ fs}$, which makes it the fastest oscillation [Fig. 2(c)]. On the other hand, the slow oscillation period is proportional to the total scattering relaxation time of electrons, which can be of few tenths of femtoseconds. But because of the argument of the exponential this slow oscillation is smoothed out quickly and it cannot take place. Only the fast oscillation survives over a few fs.

To the best of our knowledge, none of the previous non-Fourier models has shown any kind of oscillating behavior in the heat transport by either conduction-band electrons in metals or phonons in semiconductors.¹¹⁻¹⁵ As we have discussed earlier, the closest non-Fourier model to the present work is Cattaneo's model.¹¹ Based on this model, it is straightforward to show after a double Fourier transforms with respect to time and space that we can obtain an expression for the ratio of the energy density to the delta input

power at top free surface of the metal, similar to N_2 as given by Eq. (2) above. Consequently, Cattaneo's model describes the diffusive regime using the same formula in Eq. (8a). On the other hand, because of the continuous character of the model, the upper limit in the integral of Eq. (8b) is infinity, and the nondiffusive regime is described differently from the present work. We will discuss this fundamental point in the last section of the discussion.

The oscillating behavior in the energy (heat) transport that results from Shastry's formalism is a consequence of the band cutoff due to the discrete character of the lattice; the oscillations are caused by Bragg reflections of ballistically accelerated electrons at the boundaries of the first Brillouin zone. These electrons can make many round trips within the FBZ bouncing back and forth on the boundaries before they damp out due scattering mechanisms inside this zone. The ballistic electrons become afterward diffusive. This is illustrated by the difference of the amplitudes of $\delta K^</math>/ P_0 and $\delta K^>/P_0$ in Figs. 2(a) and 2(b). At short-time scales, energy and heat are mostly transported ballistically; the amplitude of the ballistic contribution is higher than the amplitude of the diffusive contribution and as the time goes by, the ballistic regime transition to a diffusive regime. For higher electron energies (high Fermi velocities), the oscillation period is shorter and the number of reflections is increased before ballistic energy transport damps out to a diffusive "thermal" regime.$

This oscillating behavior in the energy density modes can be viewed as the analogous of the Bloch oscillations of the electronic charge density in a metal subject to a uniform electric field.^{8,9} The period of conventional electron Bloch oscillations is inversely proportional to the lattice constant, while this period is proportional to the lattice constant for the energy density modes oscillations as shown in Eq. (12). Fur-

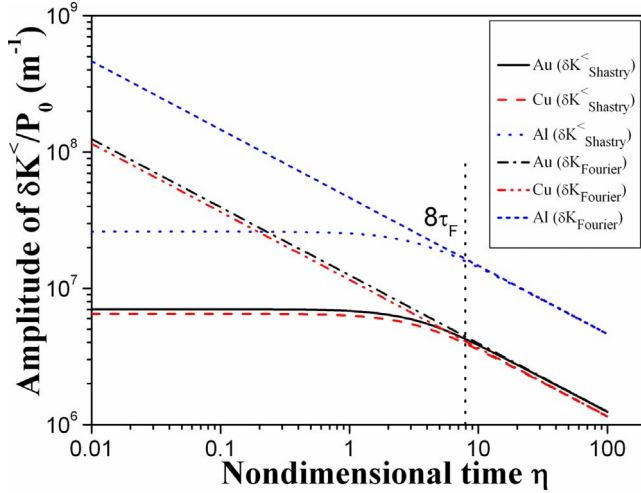


FIG. 3. (Color online) Comparison between the diffusive contribution to the total-energy density Green's function at the top free surface of the different metals and Fourier's model at room temperature.

thermore, based on the wave vector separation value $q_0 = 1/2\sqrt{D_e\tau_F}$ and the boundary of the FBZ, q_m , we can define the range of the wavelengths of electrons that contribute to the diffusive and the ballistic regimes separately. The mean-free path of an electron is defined by $\Gamma_F = v_F\tau_F$, from which is straightforward to show that q_0 will be given by $q_0 = \sqrt{3}/2\Gamma_F$. Then the wavelength of electrons that contribute to the diffusive regime is $\lambda_{\text{diff}}^e \geq \frac{4\pi}{\sqrt{3}}\Gamma_F$, and all electrons with a wavelength $2a \leq \lambda_{\text{ball}}^e \leq \frac{4\pi}{\sqrt{3}}\Gamma_F$ contribute to the ballistic regime.

In Fig. 3, we have plotted the behavior of the diffusive contribution to the energy density at the top free surface of different metals as calculated based on the present work [Eq. (8a)] as a function of the nondimensional time $\eta = t/\tau_F$, in comparison to Fourier prediction which is simply given by $\delta K_{\text{Fourier}}(t, 0) = P_0/\sqrt{4\pi D_e t}$. The diffusive contribution $\delta K^e(t, 0)$ undergoes three different behaviors. It starts as a constant at very short-time scales $t < \tau_F$, then behaves as an exponential decay up to about $8\tau_F$, from where it changes the

TABLE II. Properties of gold used in the calculation at different ambient temperatures.

Temperature T (K)	Electrical resistivity ρ ($10^{-8} \Omega \text{ m}$)	Relaxation time τ_F (fs)	Electronic thermal diffusivity D_e (m^2/s)
273	2.04	30	0.0196
169	0.592×2.04	50	0.0327
90	0.270×2.04	109	0.0712
68	0.177×2.04	167	0.1091

trend and starts following a Fourier type energy diffusion law at long-time scales with a perfect overlapping between the two predictions. Fourier's prediction is calculated analytically using Green's function method for the energy density equation.

In the next step of the analysis, the effect of the ambient temperature on the dynamics of the energy modes is addressed. The oscillating behavior is reported in Fig. 4 for the case of gold at different ambient temperatures. The values of the total scattering relaxation time τ_F are calculated from the measured values of the electrical resistivity of gold at different temperatures,²⁴ and the values of the thermal diffusivity D_e are calculated using Eq. (9). Table II summarizes these values at different temperatures.

The amplitude of the diffusive contribution to the total-energy density Green's function at the top free surface of the metal decreases and flattens by decreasing temperature. On the other hand, the oscillating behavior is still the same, independent of temperature and showing the same features [Fig. 4(b)]. This behavior was expected since the dominant oscillation period θ_F is independent of temperature as given by Eq. (12).

In Fig. 5, we report separately the behavior, as a function of the nondimensional time η , of the diffusive contribution and the sum of the ballistic and diffusive contributions to the total-energy density at the top free surface of gold at room temperature as calculated based on the present work [Eqs. (8a) and (8a) + (8b)], in comparison to Fourier's model over a long-time range of $50\tau_F$. While the ballistic contribution is

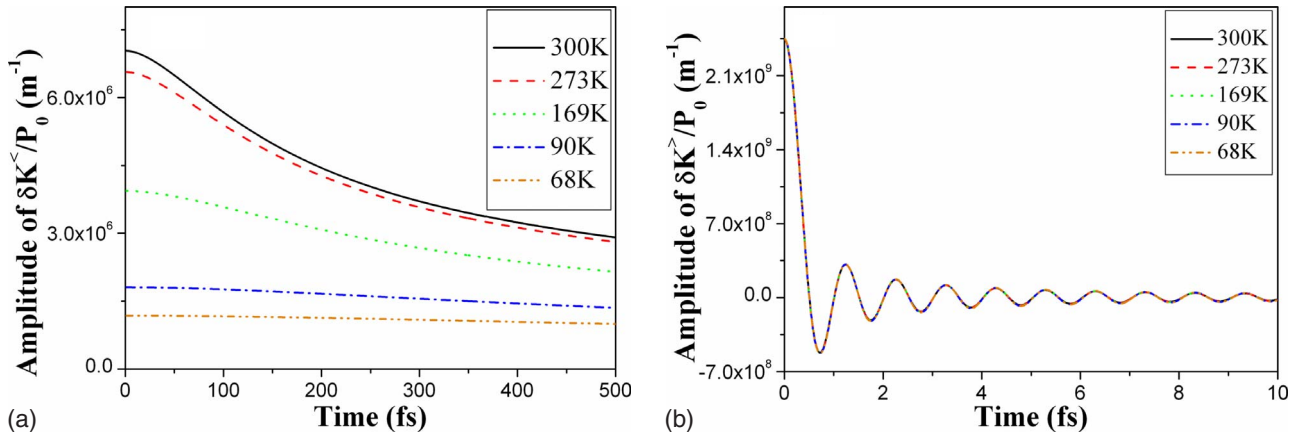


FIG. 4. (Color online) Temporal behavior of the total-energy density Green's function at the top free surface of gold at different temperatures: (a) Eq. (8a) and (b) Eq. (8b) over the first 10 fs.

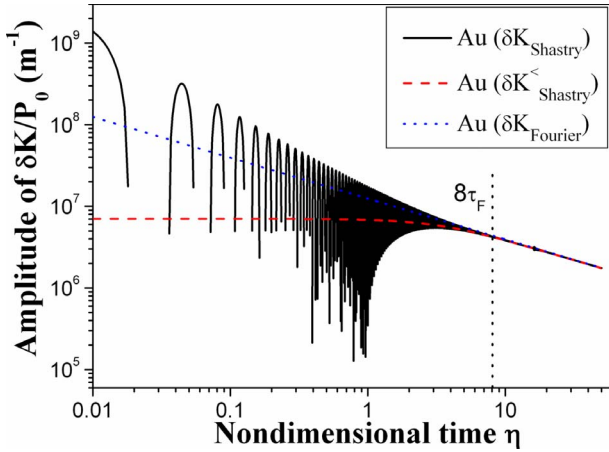


FIG. 5. (Color online) Comparison between the diffusive contribution (dashed line), the sum of the ballistic and the diffusive contributions (solid line) to the total-energy density Green's function at the top free surface of gold at room temperature, and Fourier's model (dotted line).

the dominant one at short-time scales, it becomes insignificant after about $8\tau_F - 10\tau_F$. After that moment, the total energy is transported via a diffusive regime in which case the temporal decay follows a Fourier type law.

As we have mentioned above, the closest non-Fourier model to the present work is Cattaneo's model.¹¹ This model

has some similar features as the response function N_2 . More specifically, Cattaneo's model describes the diffusive regime using the same formula in Eq. (8a). On the other hand, because of the continuous character of the model, the upper limit in the integral of Eq. (8b) is infinity, and the nondiffusive regime shows a different behavior. By following the same decomposition procedure as above, we can easily show that the nondiffusive contribution according to Cattaneo's model is given by

$$\delta K_{\text{Cattaneo}}^>(t,0) = \frac{P_0}{2\pi} e^{-t/2\tau_F} \left[\frac{\frac{\pi}{2} - \text{Si}\left(\frac{t}{2\tau_F}\right)}{\sqrt{D_e\tau_F}} \right]. \quad (13)$$

In order to shed more light on the difference between the nondiffusive contributions to the total-energy density at the top free surface of a metal, as described by Shastry's model and Cattaneo's model, we plot in Fig. 6 the results of these two models in the case of gold at room temperature for comparison. Due to the band cutoff effect in Shastry's model, the nondiffusive contribution shows an exponentially damped oscillating behavior as a function of time. On the other hand, because of the continuous character of Cattaneo's model, the oscillating behavior disappears and the nondiffusive contribution shows an exponential decay as a function of time, much faster than the diffusive contribution. The nondiffusive contribution to the total-energy density in Cattaneo's model

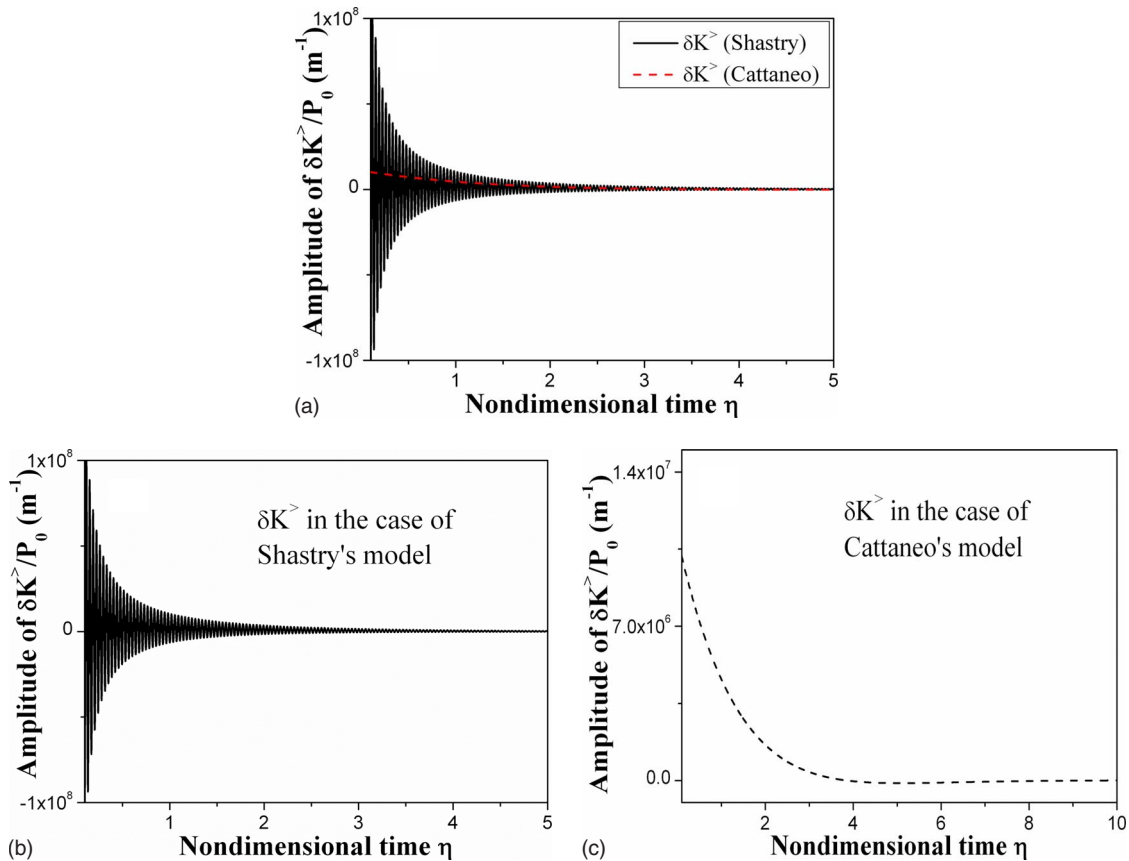


FIG. 6. (Color online) (a) Comparison between the temporal behaviors of the nondiffusive contribution to the total-energy density at the top free surface of gold at room temperature, as calculated based on Shastry's model [solid line (b)] and Cattaneo's model [dashed line (c)].

becomes insignificant after about $4\tau_F - 6\tau_F$, which is faster than the time constant decay of the nondiffusive contribution as calculated by Shastry's model.

Many authors have reported the observation of an oscillating behavior in the reflectivity change at the top free surface of semimetals using the femtosecond pump-probe transient thermoreflectance technique.²⁵⁻²⁹ Probing the relative change in the surface reflectivity is proportional to probing the change in the energy density at this surface. Nevertheless, these oscillations have been identified as due to a generation and relaxation of coherent phonon in such semimetals. The frequencies of which have been confirmed using Raman spectroscopy techniques.²⁵⁻²⁹ By consequence, these oscillations are not related to the Bloch oscillating behavior in the energy transport by conduction-band electrons in metals predicted by Shastry's formalism.

No experiment has reported such behavior in the energy density change at the free surface of metals due to electrons transport. Three main reasons can explain the lack of observation: (i) the smallness of the oscillation period (1 fs), (ii) the optical penetration depth of metals at long excitation laser wavelengths, and (iii) the convolution effect due to the laser-pulse width which smoothes out these oscillations.

A possible candidate to observe the temporal oscillating behavior in the energy transport is a metallic superlattice. As suggested by Eq. (12), the period of these oscillations is proportional to the lattice constant, which is a consequence of integration over the FBZ. It is well known however that superlattices structures are characterized by a subdivision of the electronic and phononic bands into minibands. Particularly the FBZ is divided into mini Brillouin zones of width π/d where d is the superlattice period. This spatial period d can be one to 2 orders of magnitude larger than the lattice constant a , which will increase the energy density oscillating period by the same order of magnitude and bring its value from the femtosecond regime to the picosecond regime. This latter regime can be probed by the state of the art in femtosecond laser metrology. As a matter of fact, the conventional Bloch oscillations have been only observed in superlattices structures.^{8,9}

In addition, short-pulse laser sources are in continuous development and attosecond width pulses have been developed.¹⁰ Even though many other resonance phenomena of condensed matter have to be taken into account when

using these ultrashort laser pulses, we believe that using these sources with short laser wavelengths, but are still longer than the plasmon wavelength, will be of great help to observe this fundamental oscillating phenomenon in the energy density change at the top free surface of metals and metallic superlattice structures.

IV. CONCLUSIONS

The transition between ballistic and diffusive energy transport in metals has been analyzed. An interesting temporal oscillating behavior in the energy density Green's function at the top free surface of metals is reported. This behavior in the energy transport predicted by Shastry's formalism is a consequence of the band cutoff due to the discrete character of the crystalline lattice. This leads to Bragg reflection of electrons in a metal. The oscillating behavior in the energy transport can be viewed as an energetic analogous to the conventional Bloch oscillation in the charge density of the conduction-band electrons of the metal. It is an interesting manifestation of the ballistic contribution to the energy transport that results from the electrons bouncing back and forth at the boundaries of the first Brillouin zone before they damp out into the diffusive regime due to scattering mechanisms.

Remarkably, Cattaneo's model shows similar features to Shastry's formalism. More specifically, a similar decomposition in the total-energy density at the top free surface of the metal can be made. The diffusive contribution to the energy density is described using a formula similar to Shastry's model. On the other hand, because of the continuous character of Cattaneo's model, the nondiffusive contribution shows no oscillations and it decays on a time constant even faster than the one predicted by Shastry's model.

ACKNOWLEDGMENTS

The authors are greatly thankful to B. S. Shastry for his enlightening discussions throughout this work. This work was supported by the Interconnect Focus Center, one of the five research centers funded under the Focus Center Research Program, a DARPA and Semiconductor Research Corporation program. The authors also acknowledge the support of AFOSR Thermal Transport MURI.

*younes@soe.ucsc.edu

†ali@soe.ucsc.edu

¹B. Fluegel, N. Peyghambarian, G. Olbright, M. Lindberg, S. W. Koch, M. Joffe, D. Hulin, A. Migus, and A. Antonetti, *Phys. Rev. Lett.* **59**, 2588 (1987).

²S. K. Sundaram and E. Mazur, *Nature Mater.* **1**, 217 (2002).

³P. B. Allen, *Phys. Rev. Lett.* **59**, 1460 (1987).

⁴T. Q. Qiu and C. L. Tien, *ASME J. Heat Transfer* **115**, 835 (1993).

⁵G. L. Eesley, *Phys. Rev. Lett.* **51**, 2140 (1983).

⁶J. G. Fujimoto, J. M. Liu, and E. P. Ippen, *Phys. Rev. Lett.* **53**,

1837 (1984).

⁷S. D. Brorson, J. G. Fujimoto, and E. P. Ippen, *Phys. Rev. Lett.* **59**, 1962 (1987).

⁸C. Waschke, H. G. Roskos, R. Schwedler, K. Leo, H. Kurz, and K. Köhler, *Phys. Rev. Lett.* **70**, 3319 (1993).

⁹T. Dekorsy, R. Ott, H. Kurz, and K. Köhler, *Phys. Rev. B* **51**, 17275 (1995).

¹⁰E. Goulielmakis, M. Schultze, M. Hofstetter, V. S. Yakovlev, J. Gagnon, M. Uiberacker, A. L. Aquila, E. M. Gullikson, D. T. Attwood, R. Kienberger, F. Krausz, and U. Kleineberg, *Science* **320**, 1614 (2008).

- ¹¹D. D. Joseph and L. Preziosi, *Rev. Mod. Phys.* **61**, 41 (1989).
- ¹²G. D. Mahan and F. Claro, *Phys. Rev. B* **38**, 1963 (1988).
- ¹³A. A. Joshi and A. Majumdar, *J. Appl. Phys.* **74**, 31 (1993).
- ¹⁴F. X. Alvarez and D. Jou, *Appl. Phys. Lett.* **90**, 083109 (2007).
- ¹⁵G. Chen, *Phys. Rev. Lett.* **86**, 2297 (2001).
- ¹⁶B. S. Shastry, *Rep. Prog. Phys.* **72**, 016501 (2009).
- ¹⁷D. M. Rowe, *Handbook of Thermoelectrics* (CRC, Florida, 1995).
- ¹⁸E. D. Palik, *Handbook of Optical Constants of Solids III* (Academic Press, San Diego, 1998).
- ¹⁹N. W. Ashcroft and N. D. Mermin, *Solid State Physics* (Holt, Rinehart and Winston, New York, 1976).
- ²⁰J. M. Ziman, *Electron and Phonons* (C. Press, Oxford, 1960).
- ²¹R. H. M. Groeneveld, R. Sprik, and A. Lagendijk, *Phys. Rev. B* **51**, 11433 (1995).
- ²²A. P. Kanavin, I. V. Smetanin, V. A. Isakov, Y. V. Afanasiev, B. N. Chichkov, B. Welleghausen, S. Nolte, C. Momma, and A. Tünnermann, *Phys. Rev. B* **57**, 14698 (1998).
- ²³M. Abramowitz and I. A. Stegun, *Handbook of Mathematical Functions With Formulas, Graphs and Mathematical Tables* (Dover, New York, 1972).
- ²⁴W. V. Houston, *Phys. Rev.* **34**, 279 (1929).
- ²⁵H. J. Zeiger, J. Vidal, T. K. Cheng, E. P. Ippen, G. Dresselhaus, and M. S. Dresselhaus, *Phys. Rev. B* **45**, 768 (1992).
- ²⁶H. J. Zeiger, T. K. Cheng, E. P. Ippen, J. Vidal, G. Dresselhaus, and M. S. Dresselhaus, *Phys. Rev. B* **54**, 105 (1996).
- ²⁷M. Hase, K. Mizoguchi, H. Harima, S. Nakashima, and K. Sakai, *Phys. Rev. B* **58**, 5448 (1998).
- ²⁸S. Nakashima, M. Hase, K. Mizoguchi, H. Harima, K. Sakai, S. Cho, A. DiVenere, and J. B. Ketterson, *Physica B* **263-264**, 67 (1999).
- ²⁹M. Hase, K. Ishioka, J. Demsar, K. Ushida, and M. Kitajima, *Phys. Rev. B* **71**, 184301 (2005).